Altered native stability is the dominant basis for susceptibility of α_1-antitrypsin mutants to polymerization

James A. IRVING*[1,2], Imran HAQ†[1], Jennifer A. DICKENS*, Sarah V. FAULL* and David A. LOMAS†

*Cambridge Institute for Medical Research, Department of Medicine, University of Cambridge, Wellcome Trust/MRC Building, Hills Road, Cambridge CB2 0XY, U.K.

†Wolfson Institute for Biomedical Research, The Cruciform Building, University College London, Gower Street, London WC1E 6BT, U.K.

Serpins are protease inhibitors whose most stable state is achieved upon transition of a central 5-stranded β-sheet to a 6-stranded form. Mutations, low pH, denaturants and elevated temperatures promote this transition, which can result in a growing polymer chain of inactive molecules. Different types of polymer are possible, but, experimentally only heat has been shown to generate polymers *in vitro* consistent with *ex vivo* pathological specimens. Many mutations that alter the rate of heat-induced polymerization have been described, but interpretation is problematic because discrimination is lacking between the effect of global changes in native stability and specific effects on structural mechanism. We show that the temperature midpoint (T_m) of thermal denaturation reflects the transition of α_1-antitrypsin to the polymerization intermediate, and determine the relationship with fixed-temperature polymerization half-times ($t_{0.5}$) in the presence of stabilizing additives [TMAO (trimethylamine *N*-oxide), sucrose and sodium sulfate], point mutations and disulfide bonds. Combined with a retrospective analysis of 31 mutants characterized in the literature, the results of the present study show that global changes to native state stability are the predominant basis for the effects of mutations and osmolytes on heat-induced polymerization, summarized by the equation: $\ln(t_{0.5,\text{mutant}}/t_{0.5,\text{wild-type}}) = 0.34 \times \Delta T_m$. It is deviations from this relationship that hold key information about the polymerization process.

Key words: cirrhosis, denaturation, disulfide, polymerization, serpin, stability.

INTRODUCTION

Serpins are globular proteins that predominantly act as protease inhibitors in a wide range of proteolytic cascades and environments. They are found ubiquitously in eukaryotes and in some bacterial and archaeal genomes [1,2]. The serpin native state presents an exception to Anfinsen's principle [3] as it is not the most stable form of the protein; it is a kinetically trapped intermediate whose conversion into the most stable state occurs upon proteolytic cleavage of an exposed RCL (reactive centre loop). This is the basis of the serpin inhibitory mechanism [4]. Various point mutations can perturb the barrier between native and stable states, leading to the adoption of alternative inactive forms of the serpin [5]. One such conformer is the serpin polymer, which is an ordered aggregate linearly propagated via an intermolecular linkage with a characteristic 'beads-on-a-string' appearance when visualized by EM [6]. This linkage is extremely stable: polymers can readily be extracted intact from patient samples [7], requiring mechanical disruption in the case of dense inclusions [6], and are resistant to dissociation by urea [8,9].

Serpin polymers result in a group of diseases termed the serpinopathies [10]. Many serpinopathies are the consequence of a loss of inhibitory activity, whereas others are caused by a toxic gain-of-function from the accumulation of serpin aggregates in the cell of synthesis. In α_1-antitrypsin deficiency, intracellular retention of ordered aggregates causes neonatal hepatitis and cirrhosis, and a decreased concentration of protein in the plasma underlies early-onset emphysema [11,12]. Similarly, retention of point mutants of neuroserpin within neurons results in an autosomal dominant dementia [13]; whereas the polymerization of α_1-antichymotrypsin, C1-inhibitor and anti-thrombin cause plasma deficiency of these proteins in association with emphysema, angio-oedema and thrombosis respectively [14].

Serpin polymerization can also occur under destabilizing conditions, such as at low pH [15] and in the presence of detergent [8]. In particular, induction of α_1-antitrypsin polymerization *in vitro* by the addition of chemical denaturants or through an increase in temperature has been a staple experimental technique for more than two decades [6,8]. However, biophysical [4,6,16–20] and crystallographic [21,22] studies have provided evidence that these approaches yield polymers of markedly different structural character. The stability of α_1-antitrypsin has been extensively characterized in the presence of a chemical denaturant [19,23,24], and concentrations at which the unfolding intermediate ensemble is most populated coincides with a tendency to polymerize [25]. Although there are probably commonalities between the intermediate states under various destabilizing conditions, notably only heat-generated material has been demonstrated to share a cryptic epitope with *ex vivo* pathological specimens [26,27]. For this reason, heat was chosen as the inducer for the experiments described in the present paper.

The midpoint of thermal denaturation (T_m) is one measure of the thermal stability of a protein. Analyses of several mutants have suggested an inverse trend occurs between the T_m and rate of polymerization [28,29]. In the former work, we hypothesized that this correlation related to a specific functional role played by these mutants in the opening of β-sheet A; in the latter, it was a marked departure in behaviour that was interpreted as mechanism-specific. This underlines a problem in the interpretation of

polymerization rate data. Further, several studies have drawn inferences regarding polymerization mechanism from introduced disulfides [21,22,30,31], despite the ability of disulfide bonds to stabilize a native fold by reducing local secondary structure mobility [32]. Ideally, it would be possible to decouple the effect on native state stability from the effect on mechanism. However, the extent to which native stability itself plays a role, as opposed to specific mechanistic perturbations, has not yet been demonstrated.

We undertook a detailed analysis of the effect of increased global stability of the native fold on the propensity to polymerize. Compounds known to globally stabilize serpins, sodium sulfate, sucrose and TMAO (trimethylamine N-oxide) [33–35], were characterized for their ability to alter both the midpoint of thermal denaturation and the polymerization half-time ($t_{0.5}$) of α_1-antitrypsin. It was found that increased thermal stability shared a strong direct correlation with a reduced rate of polymerization. This relationship was confirmed by a range of engineered disulfides and two point mutants of α_1-antitrypsin. Further, on the basis of our previous observation that polymer formation follows an apparent Arrhenius-type temperature dependence [36], we used a simple normalization to account for the use of different experimental temperatures, and applied it to data from five published studies. The collective results demonstrate that changes in stability of the native state, and not specific interference with molecular mechanism, are the dominant cause of mutant-based effects on polymerization.

EXPERIMENTAL

Reagents

Unless otherwise stated, reagents were obtained from Sigma, Alfa Aesar or MP Biomedicals, and numerical analyses were performed using Prism (GraphPad) and COPASI [37]. Expression media was from Formedium.

Plasmid generation for the expression of recombinant α_1-antitrypsin *in vitro*

The pQE-30 and pQE-81L plasmids (Qiagen) containing wild-type (M) α_1-antitrypsin ORF with the C232S mutation (AT$_{C232S}$) were used to express recombinant α_1-antitrypsin [38]. The C232S substitution obviates the need for a reducing agent in the assay buffer and was used as the control for *in vitro* experiments; this variant has been found to behave in an equivalent fashion to wild-type protein in previous studies (for example [16,36]). Sequential mutagenesis steps were used against the AT$_{C232S}$ background to generate the novel double-cysteine residue mutants E162C/V170C and K191C/T339C, as well as K168C/F189C, S283C/P361C and S292C/T339C that have been reported previously [21,30,31]. The point mutants K331V [29] and K335A [39] were also generated.

Expression and purification of recombinant α_1-antitrypsin

Plasmids containing AT$_{C232S}$ and mutants of α_1-antitrypsin on the C232S background were transformed into SG13009/pREP4 cells and BL21(DE3) cells (Novagen) for pQE-30 and pQE-81L-based constructs respectively. Recombinant proteins were expressed and purified as described previously [38], before buffer exchange into 20 mM Tris/HCl and 100 mM NaCl (pH 7.4) and storage at $-80\,^{\circ}$C. The resulting proteins were assessed by SDS/PAGE (4–12% gel), CD, thermal stability and for their ability to inhibit bovine α-chymotrypsin. The double-cysteine

variants were found to be predominantly in the disulfide-bonded form (>90%) by SDS/PAGE, and by their relative inability to form adducts with thiol-reactive PEG5K/maleimide and dithiodipyridine [40]. The CD spectra were essentially identical in shape, indicating no discernible effect on the structure of α_1-antitrypsin (Supplementary Figure S1 at http://www.biochemj.org/bj/460/bj4600103add.htm).

CD analysis

Far-UV spectra were obtained using a JASCO J-810 spectrapolarimeter and a 0.1-mm pathlength cell. Samples were dialysed into 10 mM NaH$_2$PO$_4$/Na$_2$HPO$_4$ (pH 7.4) and adjusted to 0.5 mg/ml before analysis, and spectra were recorded by scanning from 260 to 180 nm at a rate of 50 nm/min and averaging the replicate curves. Thermal denaturation experiments made use of a 2-mm pathlength cell, or stirred 5-mm pathlength, cuvette, with measurement of the CD signal at 225 nm and a linear increase in temperature at a rate of $1\,^{\circ}$C or $5\,^{\circ}$C/min. A thermistor probe immersed in the sample was used to directly monitor the temperature change, and the temperature profile reported by the software was adjusted as appropriate. This was of particular necessity at the higher temperature gradient.

Fluorescence-based thermal denaturation assay

The stability of α_1-antitrypsin was investigated by thermal denaturation in the presence of a $5\times$ concentration of SYPRO Orange dye solution (Life Technologies) in 25 mM NaH$_2$PO$_4$/Na$_2$HPO$_4$ and 75 mM NaCl (pH 7.4), at a final protein concentration of 0.025–0.1 mg/ml and a $20\,\mu$l volume [41]. Protein samples were heated from $25\,^{\circ}$C to $95\,^{\circ}$C at a rate of 1–$5\,^{\circ}$C/min using an Applied Biosystems 7500 quantitative real-time PCR instrument (Life Technologies). A curve describing a two-state unfolding transition [42] was fitted to the data by non-linear regression for the calculation of the transition midpoint temperatures (T_{m}).
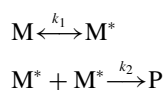
Densitometry of α_1-antitrypsin polymers

Following polymerization, α_1-antitrypsin was subjected to non-denaturing PAGE electrophoresis using a 4–12% (w/v) acrylamide Bis-Tris gel (Life Technologies). After staining with Coomassie Blue, the gel was digitized and densitometric analysis performed using GelAnalyzer 2010a software (http://www.gelanalyzer.com/). This software was also used to process the gel images presented by Gilis et al. [29].

Polymerization kinetics

An assay was previously developed in our laboratory that follows the rate of polymer formation by monitoring FRET between Ni-NTA (Ni^{2+}-nitrilotriacetic acid)-conjugated Atto-550 and Atto-647N fluorescent probes [36]. α_1-Antitrypsin was diluted to 0.2 mg/ml in 10 mM NaH$_2$PO$_4$/Na$_2$HPO$_4$ and 100 mM NaCl (pH 7.4) containing $4\,\mu$M Atto550–Ni-NTA and $4\,\mu$M Atto647N–Ni-NTA in a total volume of $20\,\mu$l. Reactions were followed for 8–16 h at $55\,^{\circ}$C, $60\,^{\circ}$C and $65\,^{\circ}$C on an Applied Biosystems 7900HT quantitative PCR instrument. FRET efficiency was calculated as the ratio between the mean of the 655–660 nm and 540–590 nm bins, and expressed as a multiple of the value recorded at the start of the experiment. Polymerization has been proposed to proceed via a simple reaction pathway, in which

a monomer (M) becomes activated (M*) before the formation of polymers (P) [28]:

$$M \xleftrightarrow{k_1} M^*$$

$$M^* + M^* \xrightarrow{k_2} P$$

although there is evidence that the process involves more than one intermediate state [36] and, at least for denaturant-activated material, dimers polymerize more rapidly than monomers [44]. Rates of unfolding can often be conveniently represented as the half-time of the conformational transition $t_{0.5}$ [45], which is related to the first-order rate constant $t_{0.5} = 0.693/k_{obs}$. We made use of this property in order to minimize assumptions and avoid model bias that could potentially arise from fitting parameters to one reaction scheme over another. A two-phase exponential function could be fitted satisfactorily to FRET progress curves by non-linear least-squares regression in COPASI [37]. The time to half-maximal signal was then determined numerically from the curve using a script in GNU Octave (https://www.gnu.org/software/octave/).

Western blot analysis of polymers using the 2C1 antibody

Recombinant AT_{C232S} or mutant α_1-antitrypsin was heated for 8 h in 20 μl reaction volumes at various temperatures in a thermal cycler. On completion, samples were snap-frozen in liquid nitrogen. Defrosted samples were resolved by non-denaturing PAGE, and subjected to Western blot analysis with binding of the 2C1 mouse monoclonal antibody overnight at 4°C [26]. HRP (horseradish peroxide)-conjugated anti-mouse antibody (1:10000 dilution; Sigma) was used as the secondary antibody. After developing, the membrane was stripped using 0.2 M NaOH for 10 min, re-blocked and incubated with rabbit polyclonal antibody (from Professor Juan Pérez, University of Málaga, Málaga, Spain), which recognizes total α_1-antitrypsin, at a 1:4000 dilution overnight at 4°C. HRP-conjugated anti-rabbit antibody (1:10000 dilution; Sigma) was used as the secondary antibody. Blots were visualized using the SuperSignal West Pico chemiluminescent substrate (Thermo Scientific).

Inhibitory activity of α_1-antitrypsin and variants

Bovine α-chymotrypsin was titrated using p-nitrophenyl acetate [47]. The stoichiometry of inhibition of AT_{C232S} and mutants of α_1-antitrypsin was determined by incubation with 0.5 μM bovine α-chymotrypsin for 30 min at room temperature (21°C) in 20 μl of assay buffer [20 mM Tris/HCl, 0.1 M NaCl, 0.1% PEG 8000 and 10 mM CaCl$_2$ (pH 8.0)]. N-succinyl-Ala-Ala-Pro-Phe-p-nitroanilide substrate (180 μl of 200 μM) was added and the absorbance at 405 nm recorded for 5 min using a ThermoMax plate reader (Molecular Devices). Linear regression was used to calculate the ratio of inhibitor required to completely abrogate enzyme activity. The association rate constant of inhibitor with enzyme (k_{ass}) was measured by reaction progress curves under pseudo-first-order conditions for 4 h at 30°C with a final concentration of 5–600 nM inhibitor, 200 μM substrate and 0.5 nM bovine α-chymotrypsin. Data analysis was performed as described previously [48].

Polymerization kinetics described in the literature

Polymerization rates were obtained from studies reported in the literature in which values had been determined from the loss of monomer as observed by native gel densitometry [29,49–51] and using intrinsic tryptophan fluorescence [28].

In the case of gel images presented by Gilis et al. [29], densitometry was performed retrospectively using GelAnalyzer 2010a software (http://gelanalyzer.com). One study used both gels and bis-ANS (4,4'-dianilino-1,1'-binaphthyl-5,5'-disulfonic acid) dye to monitor the polymerization reaction [50]. Interestingly, an examination of the rates they obtained reveals the closest linear correspondence between gel densitometry and the k_{cc} value, the 'rate of conformational change' calculated from the rapid initial increase in bis-ANS fluorescence (Supplementary Figure S2 at http://www.biochemj.org/bj/460/bj4600103add.htm). Thus the k_{cc} values presented by Cabrita et al. [52] using bis-ANS, rather than the k_{agg} values, were used as a basis for comparison (but were not included in the data used to derive the $t_{0.5}$–T_m relationship).

RESULTS AND DISCUSSION

Characterization of the pathway that underlies the serpin polymerization process is important, as it has direct relevance to toxic gain-of-function and loss-of-function phenotypes in affected individuals. Many variants of α_1-antitrypsin have been described that result in an altered tendency to polymerize [14]. To interrogate these mutants, polymerization can be induced *in vitro* by the addition of chemical denaturant or at elevated temperatures [6,8], and the production of oligomers followed by non-denaturing PAGE or spectroscopic methods such as ANS binding, tryptophan fluorescence, CD and FRET [25,28,36]. Effects on serpin stability have typically been assessed using related approaches, such as equilibrium unfolding in chemical denaturant [23] and thermal unfolding experiments [42], over a range of destabilizing conditions. It has been observed qualitatively, in different studies using disparate methodologies, that the rate of polymerization appears inversely related to the stability of the native state [28,29,33–35]. We sought to characterize this relationship in detail, at several temperatures, in an attempt to distinguish the specific effect of mutations on structural mechanism from non-specific effects on native state stability.

Thermal stability assays report the transition to a polymerization intermediate, not a globally unfolded state

Thermal denaturation experiments, using CD or environment-sensitive fluorescent dyes, such as SYPRO Orange, give information about the native stability of a protein with respect to the unfolded state [53,54], represented at its most basic by a transition midpoint temperature T_m. In contrast with the double-transition observed with denaturant-induced unfolding [23], CD-based thermal unfolding analyses of PAI-1 (plasminogen-activator inhibitor-1) [42] and α_1-antitrypsin [28] report a single transition. It may be that there is only a poorly populated thermal unfolding intermediate; alternatively, the change reported is due to other than a fully denatured state. It is noteworthy that in constant-temperature experiments, a change in CD signal is observed that precedes polymerization [36]. To characterize the transition that is reported by CD during thermal unfolding, we performed experiments using recombinant wild-type α_1-antitrypsin (AT_{WT}), and a RCL double mutant with a comparable thermal stability that polymerizes more slowly due to a greater transition-state barrier to polymer formation (L353D/A355D; denoted as AT_{P64}) [36].

For initial unfolding experiments, the temperature of each sample was increased at a rate of 1°C/min with continuous measurement of CD at 225 nm, and aliquots were periodically removed from the cuvette for analysis by non-denaturing PAGE and densitometry. A comparison of the non-denaturing gel and
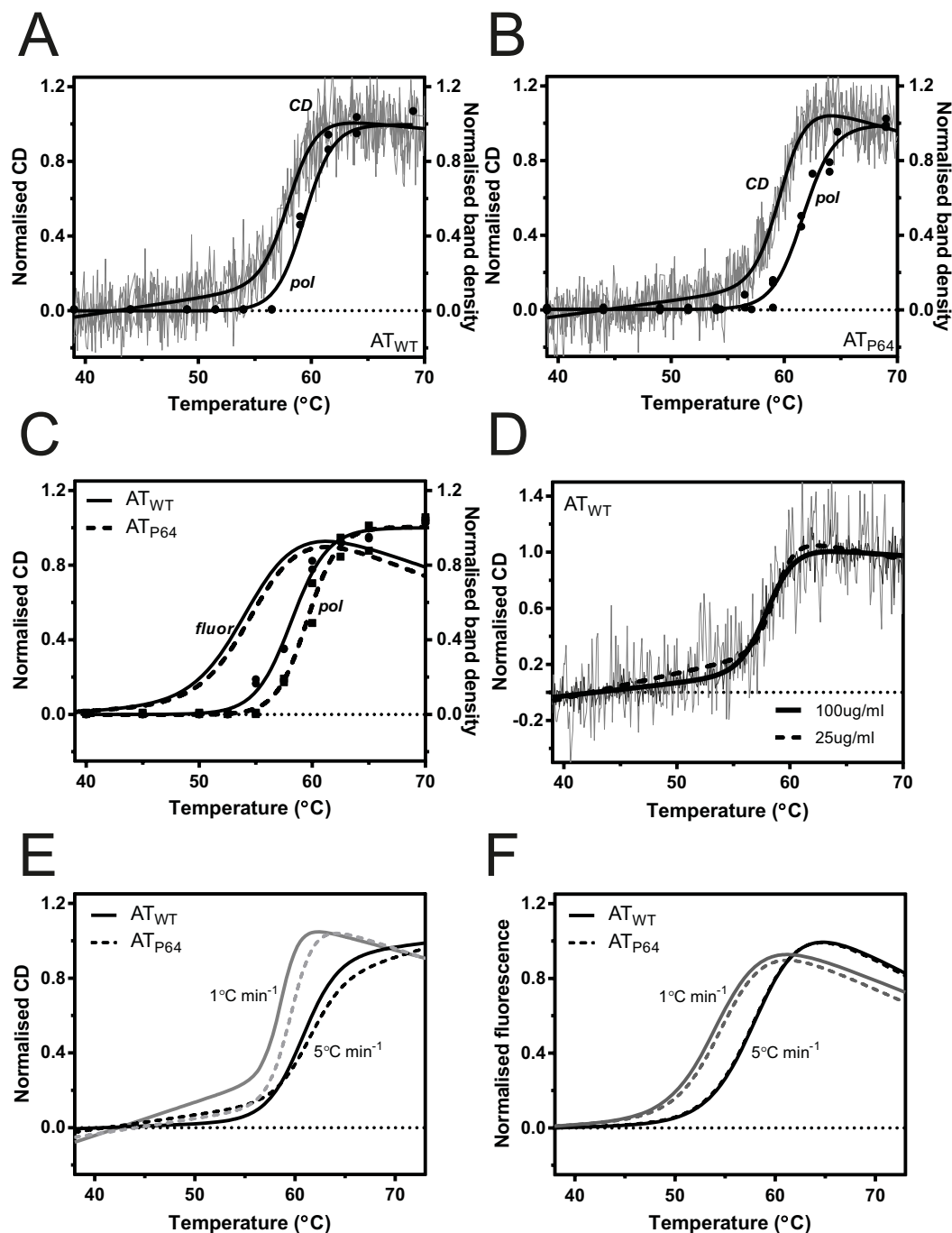
Figure 1   Characterization of thermal denaturation experiments with α_1-antitrypsin

(**A**) Recombinant wild-type α_1-antitrypsin (AT$_{WT}$) was heated at a constant rate of 1°C/min from 25°C to 95°C with continuous measurement of CD at 225 nm (grey lines). Periodically, aliquots were removed, analysed by non-denaturing PAGE (an example is shown in Supplementary Figure S3A at http://www.biochemj.org/bj/460/bj4600103add.htm), and the amount of polymer determined using densitometry (●). The result of non-linear regression analysis of the normalized data for two independent experiments, using an equation describing two-state unfolding [42], is shown as solid curves labelled 'CD' and 'pol'. (**B**) Identical experiments were repeated for a L353D/A355D mutant (AT$_{P64}$). (**C**) Summary of thermal unfolding experiments as monitored by an increase in the fluorescence of SYPRO Orange for AT$_{WT}$ (solid lines and ●) and AT$_{P64}$ (broken lines and ■) as the sample is heated at 1°C/min. Periodically, aliquots were removed and analysed by non-denaturing PAGE for the amount of polymer (● and ■). Lines show fits of an equation describing two-state unfolding. (**D**) The normalized CD data from thermal unfolding experiments of two concentrations of AT$_{WT}$ (25 and 100 μg/ml) at a constant rate of 1°C/min are shown. The thick lines indicate the fit of an equation describing two-state unfolding. (**E**) AT$_{WT}$ (solid lines) and AT$_{P64}$ (broken lines) were heated at 1°C/min (grey lines) and 5°C/min (black lines), with unfolding monitored by the change in CD at 225 nm. Lines show the curve fit to three independent experiments. (**F**) AT$_{WT}$ (solid lines) and AT$_{P64}$ (broken lines) were heated at 1°C/min (grey lines) and 5°C/min (black lines), with unfolding monitored by the change in SYPRO Orange fluorescence. Lines show the curve fit to three independent experiments.

CD progress curve for AT$_{WT}$ shows that the change in CD signal precedes the appearance of polymer on the gel, with a calculated midpoint difference of 1.4 ± 0.4°C (Figure 1A,

Supplementary Figure S3A at http://www.biochemj.org/bj/460/bj4600103add.htm, and Table 1). As α_1-antitrypsin polymers are known to be extremely stable and do not dissociate even in the

Table 1   Transition midpoint temperatures (T_m) of AT$_{WT}$ and AT$_{P64}$ calculated from thermal denaturation curves

Samples were monitored for changes in CD, density of polymer bands resolved by non-denaturing PAGE, and SYPRO Orange fluorescence (Dye) during heating at a fixed rate. Curves describing two-state unfolding [42] were fit to the data from two to four independent experiments. Individual curve midpoints $\pm$ S.D. are shown.

Reporter	Concentration (μg/ml)	Heating rate (°C/min)	T_m (°C) AT$_{WT}$	AT$_{P64}$
CD	100	1	58.1 $\pm$ 0.2	59.8 $\pm$ 0.1
PAGE	100	1	59.5 $\pm$ 0.3	61.7 $\pm$ 0.4
CD	25	1	58.5 $\pm$ 0.5	–
CD	25	5	60.9 $\pm$ 0.2	61.3 $\pm$ 0.6
Dye	100	1	55.0 $\pm$ 0.5	55.2 $\pm$ 0.5
PAGE (+ dye)	100	1	58.2 $\pm$ 0.1	59.5 $\pm$ 0.5
Dye	100	5	58.5 $\pm$ 0.1	58.5 $\pm$ 0.1

presence of high concentrations of urea [9,55], this disparity is not the result of dissociation during electrophoresis. Indeed, for the AT$_{P64}$ mutant, the appearance of polymer was further delayed on the gel, with a polymer midpoint 1.9 ± 0.4°C greater than the CD transition (Figure 1B, Supplementary Figure S3A and Table 1). As AT$_{P64}$ has been shown to exhibit an increased energetic barrier late in the polymerization pathway [36], this is consistent with CD reporting foremost an early activation step that precedes polymerization. The thermal melt was also repeated using SYPRO Orange, a dye whose fluorescent quantum yield increases substantially in a non-polar environment, and has been used previously with α_1-antitrypsin [36]. Again, the increase in fluorescence preceded polymer formation, in this case by an increased margin of 3.2 ± 0.5°C and 4.4 ± 0.7°C for the wild-type and AT$_{P64}$ mutant respectively (Figure 1C and Table 1).

Unfolding is a first-order process, whereas polymerization is concentration-dependent. When the CD denaturation assay was repeated at a 4-fold lower concentration, an almost identical value for T_m was obtained (Figure 1D and Table 1), as was the case when the SYPRO Orange reporter was used (Supplementary Figure S3C and Table 1). This insensitivity to concentration is consistent with first-order behaviour. However, different midpoints were obtained by both methods when the experiments were repeated at a higher heating rate of 5°C/min (Figures 1E and 1F, and Supplementary S3B), indicative of an unfolding process under kinetic, rather than thermodynamic, control. Such a scenario can arise even when the recorded change reflects a reversible process, if there is competition from a subsequent kinetically controlled step [56]. The association of monomers to form polymers, whose stability against dissociation has long been recognized [8,55,57], certainly would be an example of this.

Correspondingly, conditions under which intermolecular association would be expected to play a less prominent role show convergence of CD-reported T_m values for AT$_{WT}$ and AT$_{P64}$: a difference of 0.4°C at 25 μg/ml and 5°C/min compared with 1.7°C at 100 μg/ml and 1°C/min (Table 1). Indeed, when AT$_{WT}$ was subjected to thermal unfolding up to the transition midpoint temperature, and subsequently cooled, the CD measurement returned to an intermediate value, suggesting a partially reversible unfolding event (Supplementary Figure S4 at http://www.biochemj.org/bj/460/bj4600103add.htm).

The detectable separation of the spectroscopic changes from polymerization indicates that the branch of the pathway that yields polymers is rate-limiting. Thus it is apparent that these two common methods of evaluating thermal stability report the transition to a thermal polymerization intermediate state, in a

manner that is influenced by, but not contingent on, the subsequent formation of polymers.

Additive-mediated stabilization of α_1-antitrypsin against intermediate formation

Osmolytes exert non-specific global effects on protein integrity, primarily by altering solvent behaviour or through unfavourable interactions with the protein backbone, favouring a compact folded state [58]. For α_1-antitrypsin and neuroserpin, the result is a reduced rate of polymerization and an increase in observed T_m values [33–35]. Considering this general trend and the nature of the unfolding transition measured using CD, it has been suggested that this effect is elicited by stabilization of the serpin native state [34,35]. We set out to use this system to establish the baseline relationship between generic changes in native state stability, reflected partly in the value of T_m, and the rate of α_1-antitrypsin intermolecular association. TMAO was used due to its marked stabilization of α_1-antitrypsin at high concentrations [35], as well as representatives of two other classes of osmolyte, sucrose (a polyol) and sodium sulfate (a kosmotropic salt). AT$_{C232S}$, in which the free cysteine is mutated to a serine, was the background used for later mutagenesis and so was used in subsequent experiments.

Thermal unfolding experiments of AT$_{C232S}$ were conducted in the presence of the SYPRO Orange reporter dye. Owing to our observation of the kinetic-biased nature of the unfolding curves, we did not directly infer thermodynamic parameters from them. Several TMAO concentrations between 0 and 3.5 M (Figure 2A, left-hand panel), 0 to 2 M sucrose (Figure 2A, middle panel) and 0 to 0.8 M sodium sulfate (Figure 2A, right-hand panel) were used. As expected, there was a progressive shift of the melting curve to higher transition temperatures in the presence of higher levels of TMAO. Despite their different chemical properties, the other two stabilizing compounds showed a qualitatively similar effect on α_1-antitrypsin stability, albeit at substantially different concentrations. The unfolding curves were accommodated well by a two-state equation, from which T_m values could be calculated. For all three additives, the T_m values showed a clear linear dependence on osmolyte concentration (Figure 2B), consistent with increasing stability of the native state against formation of a partially unfolded state. The stabilization by TMAO, sucrose and sodium sulfate was 3.5 ± 0.2°C/M, 9.0 ± 0.1°C/M and 16.3 ± 0.3°C/M respectively.

The effect of stabilizing compounds on polymerization half-time

For the determination of the rate of polymerization, a FRET-based approach was used to monitor intermolecular association. This assay uses nitrilotriacetic acid-conjugated fluorescent dyes that bind to an N-terminal His$_6$ affinity tag and report an increase in proximity between interacting monomers through an increase in FRET efficiency [36]. The polymerization of AT$_{C232S}$ was followed in the presence of the same range of concentrations of co-solute as detailed above, at 55°C, 60°C and 65°C with 0.2 mg/ml protein and 4 μM reporter dye. The resulting progress curves were well described by a two-phase exponential association function. Although convenient for subsequent analyses, this concordance is not expected to be a true reflection of the polymerization mechanism; in particular, it does not explain the presence of a concentration-dependent behaviour [28,36]. We preferred the use of the polymerization half-time ($t_{0.5}$) as a simple descriptor for the curves, in order to avoid assumptions about the reaction pathway inherent in more complex treatments. Additionally, this facilitated comparison with other studies, as polymerization rates
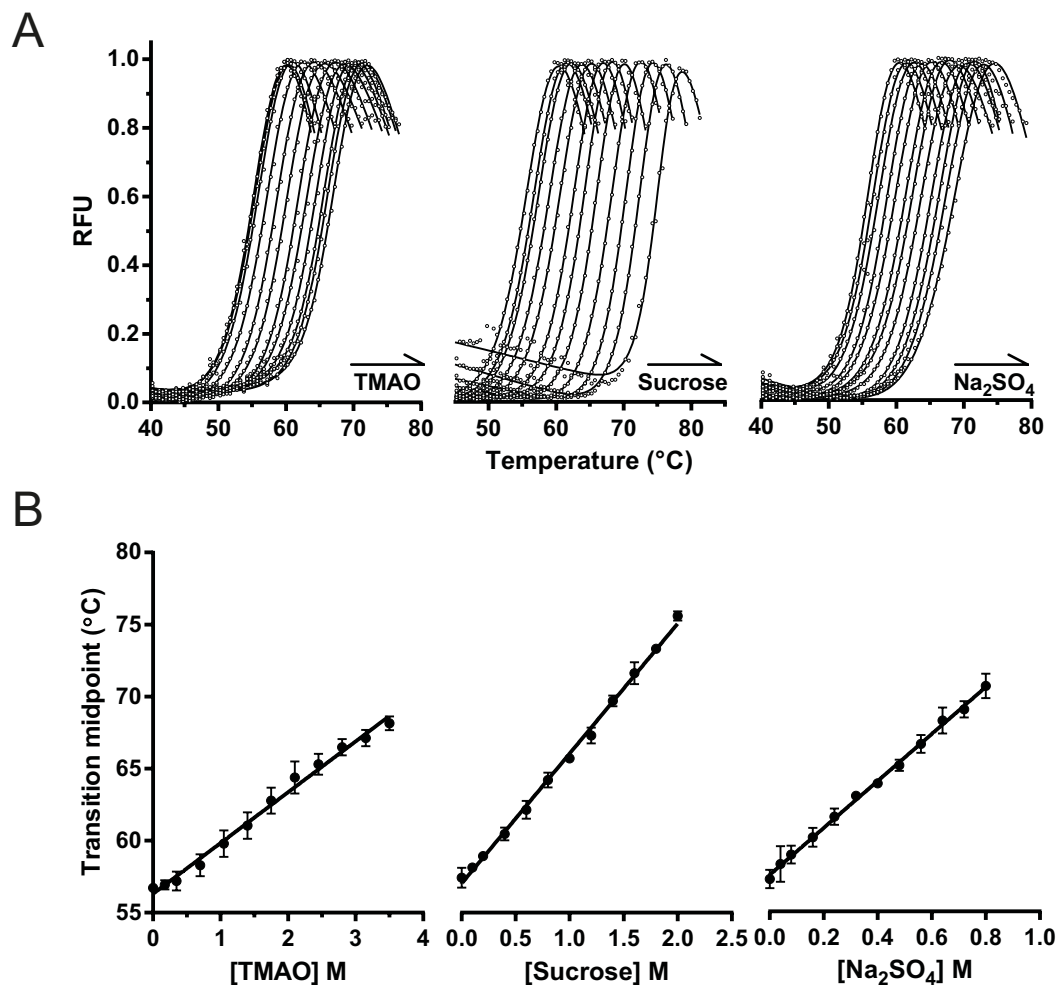
Figure 2   The effect of TMAO, sucrose and sodium sulfate on thermal transition midpoints of α_1-antitrypsin

AT_{C232S}, at a concentration of 0.1 mg/ml, was heated at a rate of 1 °C/min from 25 °C to 95 °C in a buffer containing 25 mM NaH_2PO_4/Na_2HPO_4, 75 mM NaCl (pH 7.4) and 5× SYPRO Orange in the presence of 0–3.5 M TMAO (left-hand panels), 0–2 M sucrose (middle panels) and 0–0.8 M sodium sulfate (right-hand panels). (**A**) The resulting normalized curves of fluorescence of SYPRO Orange, calculated from the mean of four independent experiments, were fitted to an equation describing two-state unfolding, with progressive stabilization evident at increasing additive concentrations. (**B**) The midpoint temperatures showed a linear dependence on additive concentration. Error bars represent the S.D. for four independent measurements.

have typically been reported in the literature either as half-times or first-order rate constants, such as k_{obs}, which are related to one another by the simple transformation $t_{0.5} = 0.693/k_{obs}$. The parameterized curves were therefore subsequently used for the numerical determination of the half-time of the polymerization. Indicative values are presented in Table 2.

The relationship between rates of polymerization and T_m values

To compare the effect of the co-solutes on polymerization, the linear relationship between stabilizer concentration and T_m value (Figure 2B) was used to represent the data on a common scale. As the concentration of each co-solute increased, so too did the resulting values of T_m and $t_{0.5}$, and the natural logarithm of the $t_{0.5}$ values showed a strong positive dependence on T_m (Figures 3A–3C). We had described previously an Arrhenius-type temperature dependence for polymerization [36], and had found the thermal unfolding pathway to reflect a reversible transition followed by a subsequent rate-limiting irreversible process. We were therefore able to globally fit each multiple-temperature

dataset to an equation that describes a kinetically controlled (non-equilibrium) process [56,59]:

$$t_{0.5,\mathrm{stab}} = 0.693/\exp^{(-E_{\mathrm{act,app}}/R(1/T-1/T^{\star}_{\mathrm{stab}}))} \tag{1}$$

where $E_{\mathrm{act,app}}$ is the apparent activation energy for the polymerization reaction, R is the universal gas constant, T is the experimental temperature in K, and T^{*}_{stab} is a reference temperature at which the polymerization rate of the stabilized preparation is 1 s^{-1}, derived from the apparent T_m value by $T^{*}_{\mathrm{stab}} = aT_m$, where a is a scaling factor that is optimized during curve fitting.

Despite marked chemical differences between these compounds, the resulting curves for TMAO, sucrose and sodium sulfate reflected a remarkable correspondence (Figures 3A–3C, broken lines). Deviations occurred essentially at the highest concentrations, where the distinct chemical natures of the compounds are more likely to exert an effect. The optimized values of $E_{\mathrm{act,app}}$ and a were correspondingly almost identical for each compound (Supplementary Table S1 at http://www.biochemj.org/bj/460/bj4600103add.htm); all data were therefore

Table 2 Representative polymerization half-lives in the presence of different solutes

AT_{C232S} was heated at a constant temperature in the presence of several different concentrations of stabilizing additives, and polymerization was monitored by FRET. The time taken to reach a half-maximal signal $\pm$ S.D. for a subset of these experiments is shown.

| Additive | Temperature | | | | | |
| | 55°C | | 60°C | | 65°C | |
	Concentration (M)	$t_{0.5} \times 10^{-2}$ s	Concentration (M)	$t_{0.5} \times 10^{-2}$ s	Concentration (M)	$t_{0.5} \times 10^{-2}$ s
None	–	4.28 ± 0.13	–	0.60 ± 0.06	–	0.23 ± 0.02
TMAO	2.9	97.9 ± 6.0	3.5	19.2 ± 0.6	3.5	4.7 ± 0.1
Sucrose	1.1	64.2 ± 27.0	1.7	119.0 ± 16.3	2	67.3 ± 5.3
Sodium sulfate	0.8	180.1 ± 17.0	0.8	71.7 ± 2.8	0.8	11.9 ± 4.1

combined, with a global parameter optimization yielding values of 320 ± 4 kJ/mol and 1.05 for $E_{\mathrm{act,app}}$ and a respectively.

This Arrhenius-type behaviour could also be exploited to normalize the data collected at different temperatures; subtraction of the $\ln(t_{0.5})$ value obtained in the absence of co-solute at each experimental temperature ($t_{0.5,0M}$) revealed an excellent overlap between the data collected at all three temperatures (Figure 3D). For the sake of comparison with other studies, the results of the thermal denaturation assay were calculated as ΔT_{m} values, relative to that of protein in the absence of co-solute. Linear regression of the combined data for the three osmolytes at the three different temperatures yielded the relationship:

$$\ln(t_{0.5,\mathrm{stab}}) - \ln(t_{0.5,0M}) = 0.34(\pm 0.1) \times \Delta T_{\mathrm{m}} \qquad (2)$$

with $t_{0.5,0M}$ representing the half-time and $T_{\mathrm{m,0M}}$ representing the midpoint of thermal denaturation in the absence of co-solute. This represents an approximation of eqn (1), which, despite describing a hyperbolic relationship, is essentially linear in nature over the range of temperatures considered (Figures 3A–3C). If we compare the natural logarithm of $t_{0.5,\mathrm{stab}}$ of a stabilized preparation, with respect to that of the control, $t_{0.5,0M}$, the result is independent of experimental temperature T. It can be shown that, from eqn (1):

$$\ln(t_{0.5,\mathrm{stab}}) - \ln(t_{0.5,0M}) \approx (E_{\mathrm{act,app}}\Delta T_{\mathrm{m}})/(aRT_{\mathrm{m,0M}}^2) \qquad (3)$$

and, substituting the values determined above, $E_{\mathrm{act,app}}/(aRT_{\mathrm{m,0M}}^2) = 0.34$ (see the Supplementary Online Data for details at http://www.biochemj.org/bj/460/bj4600103add.htm). It would be interesting to see whether this form of analysis can be applied to other serpins by substitution of the relevant parameters.

Thus for the non-specific stabilization elicited by these compounds, there is a strikingly direct correspondence between thermal stability, as reported by the thermal denaturation assay, and polymerization kinetics.

Stabilized α_1-antitrypsin variants

Osmolytes exert non-specific global effects on protein integrity primarily through manipulation of solvent behaviour or through unfavourable interactions with the protein backbone, promoting a compact folded state [58]. As mutations affect protein behaviour directly, we sought to determine whether known, and novel, mutations result in a comparable relationship between stability and the rate of polymer formation. Previously, destabilizing mutations in the shutter domain and proximal and distal hinges of the RCL have been found to increase the rate of polymerization [28]. Further, disulfides that restrict the movement of mobile

elements of the serpin scaffold have been found to interfere with polymerization [21,22,30,31,60]. It is evident that, in some cases, this interference manifests as reduction in, rather than loss of, the ability to polymerize [22,31]. Seven variants were considered (Figure 4A): a mutant to prevent the release of strand 1C from the C-sheet (283–361) [30]; a mutant to prevent release of strand 5A from the A-sheet (292–339) [21]; a mutant to stabilize the C-terminus of the F-helix (162–170); a mutant to prevent opening of β-sheet A (191–339); a mutant of the disulfide tethering the F-helix to strand 3A (168–189) [31]; and two thermostable point mutants (K335A and K331V) [29,39].

Serpins rely on differences in the energy of two conformational states during the inhibition of a target protease, and residual inhibitory activity provides an alternative function-specific measure of native stability relative to the inserted six-stranded form of the protein (Table 3). As RCL insertion is an obligate component of the inhibitory mechanism, 191–339 was essentially non-inhibitory; its SI was consistent with approximately 4% of the material lacking the disulfide bond. Activity against bovine α-chymotrypsin was reduced in the K331V and 168–189 forms, but was similar to the AT_{C232S} control for the other variants. All variants showed moderate to pronounced enhancement of thermostability in a SYPRO-based thermal melt assay (Table 3).

Polymers recognized by the 2C1 monoclonal antibody can form in the presence of stabilizing disulfide bonds

Preliminary experiments revealed that 283–361 and 292–339 were able to polymerize, despite previously published observations that they were incapable of doing so [21,30]. Polymerization can occur by more than one pathway; conditions such as the use of heat, chemical denaturants and mutations can consequently alter the configurations of the resulting polymer [22,27]. We therefore made use of the 2C1 antibody, which provides a means to identify α_1-antitrypsin polymers generated *in vitro* that are non-orthologous to those isolated from patients [26,27]. The α_1-antitrypsin variants were heated at 60°C for 8 h, the polymers separated by non-denaturing PAGE, and then visualized by Western blotting. After heating, all variants had predominantly formed higher molecular mass species, with the exception of 191–339, which due to an absence of detectable material, had most probably precipitated from solution (Figure 4B, upper panel). In order to determine whether any mutations altered the polymerization pathway, we compared recognition of the mutants with the 2C1 antibody. AT_{C232S}, 292–339, 283–361, 162–170 and K335A formed 2C1$^+$ polymers at 60°C (Figure 4B, lower panel). In contrast, the 168–189 variant produced predominantly 2C1$^-$ polymers, suggesting that it causes the reaction to
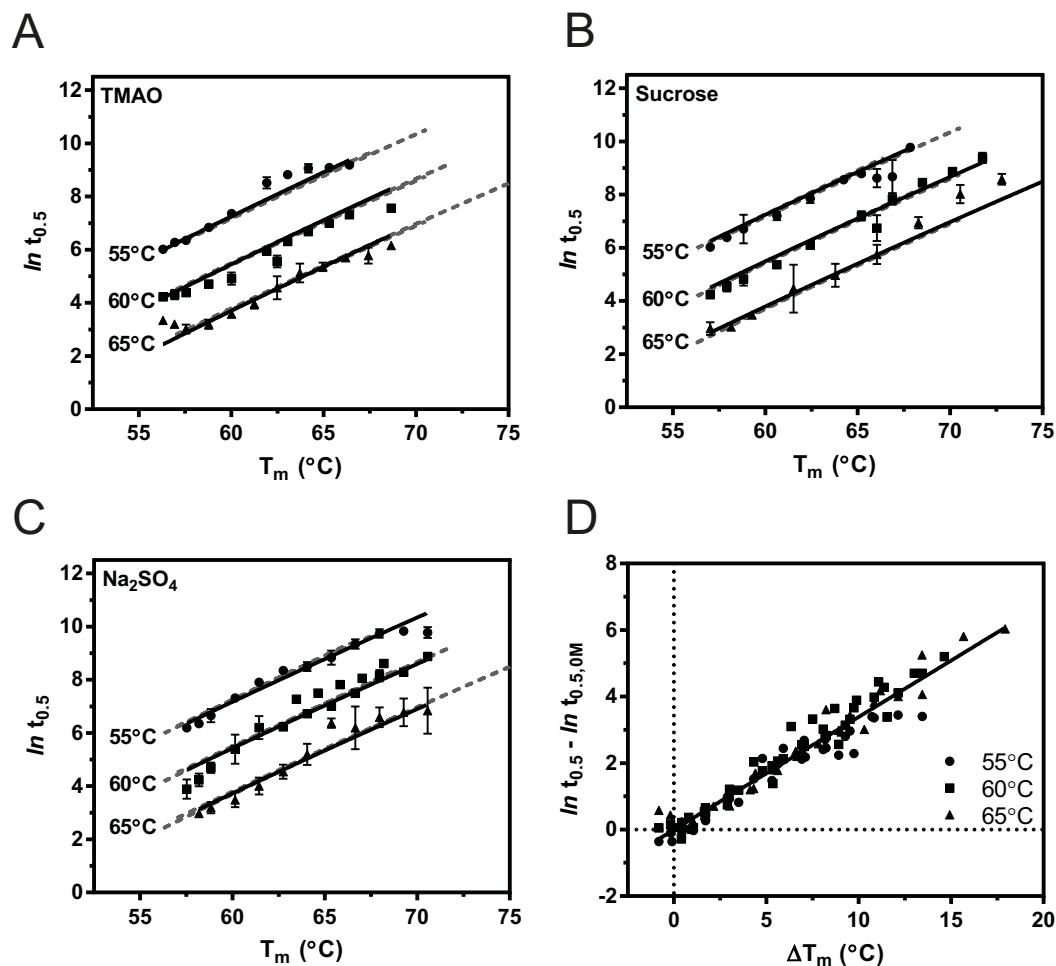
Figure 3   The rate of polymerization in the presence of additives

Polymerization was monitored using a FRET-based assay for AT_{C232S} in the presence of (**A**) TMAO, (**B**) sucrose and (**C**) sodium sulfate at 55 °C, 60 °C and 65 °C. Additive concentration was converted into T_m values based on the linear relationships shown in Figure 2, permitting direct comparison of the three additives on a common scale (abscissa). The half-time of polymerization, $t_{0.5}$, in the presence of the osmolytes, was obtained by fitting progress curves to a two-phase exponential equation for numerical derivation of the time at which the signal reached 50 % of the range of the experiment. The data at all temperatures were globally fit to an equation describing the effect of experimental temperature, T_m and the activation energy of an irreversible step, on the rate of polymerization [56,59]. For comparison, the results of the regression with other co-solutes are shown as broken lines. (**D**) The half-times for all co-solutes ($t_{0.5}$) were normalized by subtracting the natural logarithm of the value for the AT_{C232S} control ($t_{0.5,0M}$) at each temperature, resulting in a superimposition of all data presented in (**A**–**C**). These combined data were used to perform a linear regression analysis, as described in the text. Results are means $\pm$ S.E.M. from at least four independent experiments.

favour a different pathway. Hence four of these mutants failed to prevent any structural rearrangement prerequisite to the polymerization mechanism. As disulfide bonds can result in an overall stabilization of the native fold by reducing local secondary structure mobility [32], we sought to determine whether these mutants affect polymerization through specific or non-specific effects.

The effect of stabilizing mutations on the rate of polymerization

Using the FRET-based assay, the times taken to reach half-maximal polymerization signal were determined for AT_{C232S} and stabilized variants at 55 °C, 60 °C and 65 °C. The results are shown in Table 4. At 55 °C, all of the mutants considered demonstrated a 1.5- to 25-fold delay with respect to the AT_{C232S} control, whereas at 65 °C 283–361, 292-339 and K331V were comparable with the control. We have previously shown Arrhenius-type behaviour for α_1-antitrypsin polymerization in the experimental

temperature range [36]. When $\ln(t_{0.5})$ was plotted against the reciprocal absolute temperature, this behaviour was found to hold for these stabilized mutants as well (Figure 5A). Activation energies obtained from the resulting slopes revealed that, despite conferral of a marked increase in thermal stability, all but two of the mutants failed to significantly alter the kinetic barrier to polymer formation (Figure 5B and Table 4), including the most polymer-resistant variant K335A. This serves to highlight that resistance to polymerization does not of itself indicate interference with the irreversible (and thus kinetically determined) component of the pathway.

The collective stability-polymerization profile of the mutants was compared with that determined for the wild-type protein in the presence of osmolytes. As shown in Figure 5(C), there is a reasonable overall correspondence between the two, but with notable deviations. Three types of behaviour are evident.

(i) 168–189, K331V and K335A behave in a similar manner to wild-type protein stabilized by osmolytes. This suggests they have a native state with an increased thermodynamic stability,
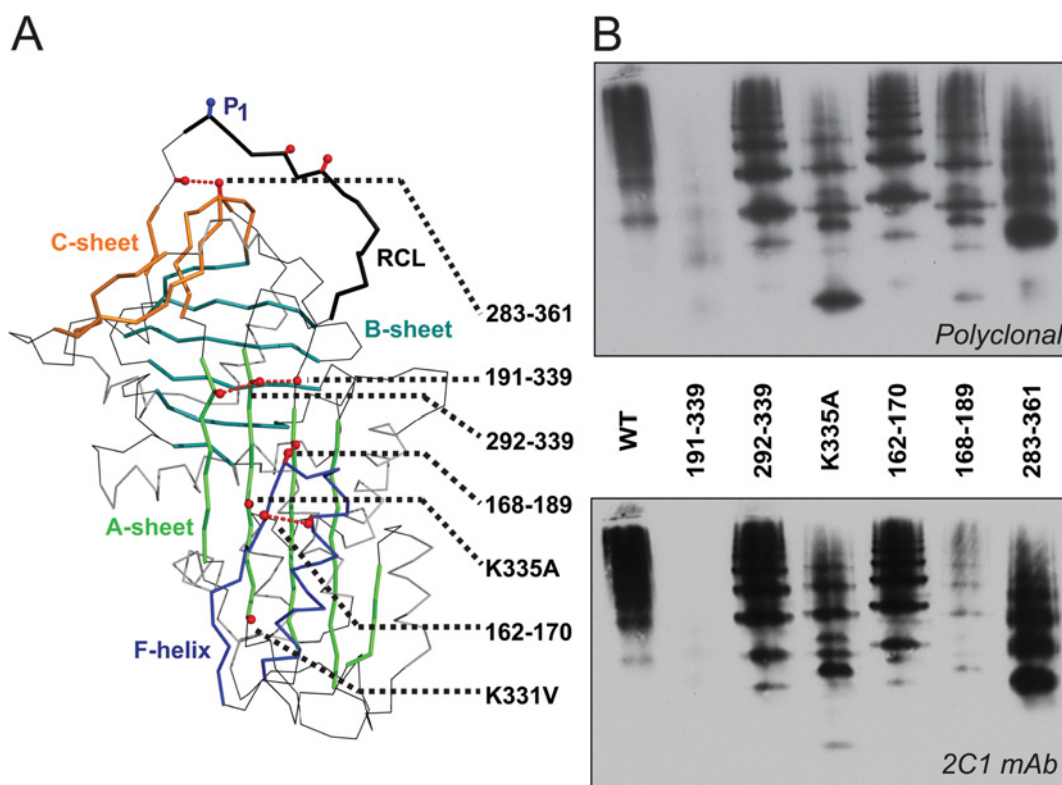
Figure 4   Disulfide-stabilized variants of α_1-antitrypsin

(**A**) The location of stabilizing mutations characterized in the present study are indicated against a cartoon representation of AT$_{C232S}$ α_1-antitrypsin (prepared using PyMOL (http://www.pymol.org) and PDB code 1QLP [62]). (**B**) AT$_{C232S}$ and mutants were heated at 60°C for 8 h and separated by non-denaturing PAGE. Western blot analysis was performed using the 2C1 anti-pathogenic polymer antibody (lower panel) before stripping and re-probing with a total α_1-antitrypsin antibody (upper panel).

Table 3   Biophysical and biochemical characteristics of recombinant wild-type and mutants of α_1-antitrypsin

Variants were assessed for their midpoint of denaturation, stoichiometry of inhibition (SI) and association rate constant (k_{ass}) against bovine α-chymotrypsin. The results are the mean of at least three independent experiments. Rows labelled 'reduced' are for protein treated with 100 mM 2-mercaptoethanol.

Variant	T_m (°C)*	SI†	k_{ass} (M^{-1}·s^{-1})	$k_{ass} \times$ SI
AT$_{C232S}$	55.0	1.1 ± 0.02	$1.5 \pm 0.2 \times 10^6$	1.5×10^6
Disulfide mutants				
162–170	64.5	1.0 ± 0.02	$1.6 \pm 0.3 \times 10^6$	1.6×10^6
162–170 (reduced)	55.0	1.0 ± 0.05	$1.5 \pm 0.2 \times 10^6$	1.5×10^6
168–189	67.5	8.5 ± 0.4	$4.2 \pm 0.7 \times 10^3$	3.6×10^4
168–189 (reduced)	56.0	1.2 ± 0.03	$1.0 \pm 0.1 \times 10^6$	1.2×10^6
191–339	59.5	27 ± 1.4	$2.0 \pm 0.4 \times 10^4$	5.4×10^5
191–339 (reduced)	55.0	1.0 ± 0.03	$0.9 \pm 0.04 \times 10^5$	0.9×10^5
283–361	60.5	1.0 ± 0.01	$1.3 \pm 0.1 \times 10^6$	1.3×10^6
283–361 (reduced)	56.5	1.0 ± 0.04	$1.4 \pm 0.6 \times 10^6$	1.4×10^6
292–339	61.5	1.0 ± 0.03	$1.4 \pm 0.3 \times 10^6$	1.4×10^6
292–339 (reduced)	57.0	1.0 ± 0.03	$1.7 \pm 0.04 \times 10^6$	1.7×10^6
Strand 5A/F-helix				
K331V	59.0	3.9 ± 0.2	$1.0 \pm 0.1 \times 10^6$	3.9×10^6
K335A	70.0	1.0 ± 0.02	$0.9 \pm 0.1 \times 10^6$	0.9×10^6

*All standard errors were less than precision of the technique on the instrument used (± 0.5°C).

†Standard errors were calculated by regression of a transformed linear equation with the intercept at the abscissa as a parameter.

consistent with conclusions drawn from denaturant-mediated unfolding of the latter two variants [29,50]. However, the relative stability of the thermal unfolding intermediate appears unaffected

with respect to the transition state of the kinetically controlled step (Figures 5D, *1*).

(ii) 292–339 and 162–170 increase the overall $t_{0.5}$ value, but not to the extent predicted from their ΔT_m values. This would be consistent with a mode of action in which the native state is only partially stabilized. The thermal unfolding intermediate and kinetic transition states are also destabilized to a slightly greater (292–339) or lesser (162–170) extent (Figure 5D, *2*), as seen by a modest change in E_{act} value (Table 4).

(iii) The restraints imposed by the 283–361 mutant present the greatest energetic barrier to polymer formation, with an E_{act} value 1.6-fold higher than the control (Table 4). At 55°C and 60°C, 283–361 has a greater $t_{0.5}$ value than predicted from the value of ΔT_m (Figure 5C). Thus it probably both stabilizes the native state and destabilizes the transition state of the irreversible step, increasing the kinetic barrier to polymerization (Figure 5D, *3* and *4*).

Conformational mobility of the RCL is clearly enhanced in the transition state of the irreversible step, as shown by its destabilization in the presence of the 283–361 and 292–339 disulfides. As these mutants are still able to form polymers (Table 4) that are recognized by the 2C1 antibody (Figure 4B), this loss of mobility merely increases the kinetic barrier to polymerization, rather than preventing it altogether. We note that these observations differ from single-temperature studies that concluded an absolute requirement for mobility of the 283–361 and 292–339 regions during polymerization [21,30].

In addition, as the rate of polymerization is strongly coupled to the thermal stability of the α_1-antitrypsin native state, it is deviations from the expected profile that provide information about effects on irreversible changes along the polymerization
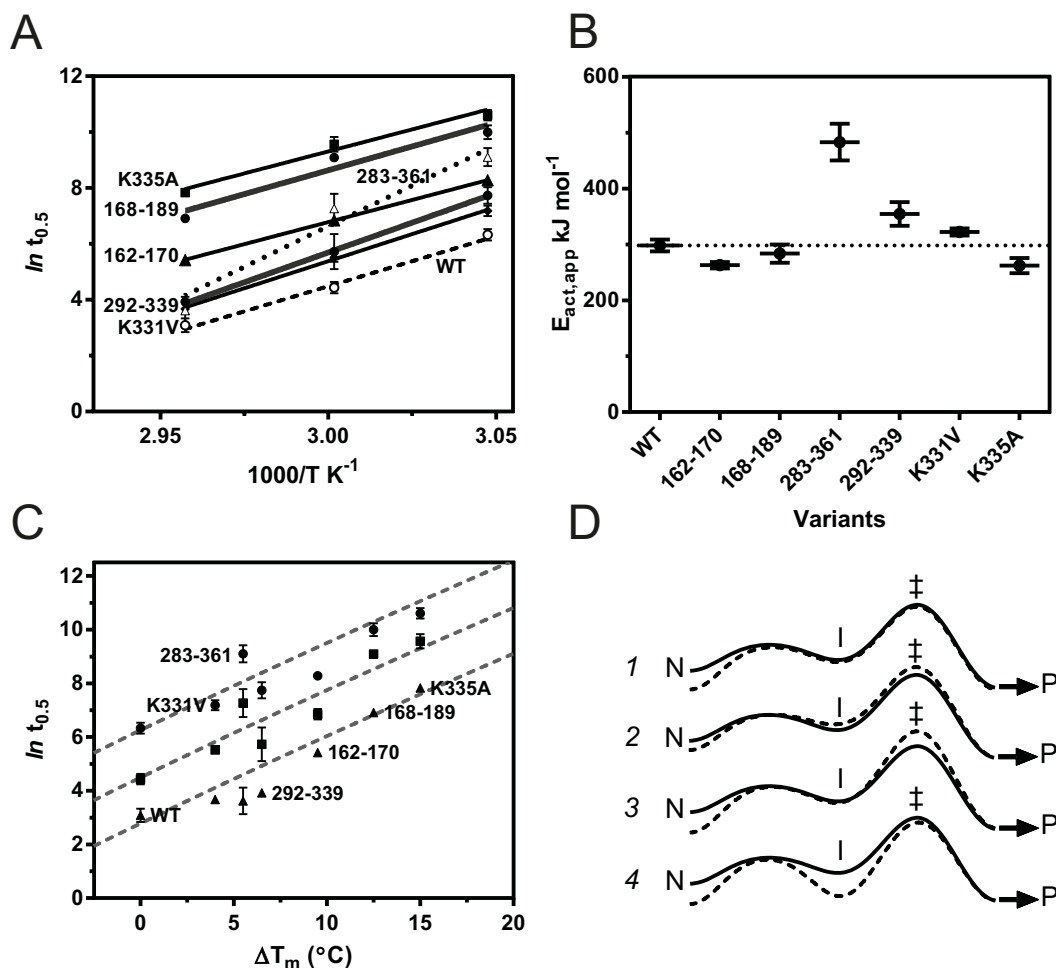
Figure 5   Relationship between mutant thermal stability and the rate of polymerization

Polymerization of AT_{C232S} and the stabilized mutants was monitored using the FRET-based assay. (**A**) The relationship between the natural logarithm of the half-times, and the inverse absolute temperature at which they were determined, is presented. Based on the Arrhenius-type temperature dependence, linear regression analysis permitted the derivation of E_{act} values. The AT_{C232S} control is shown as a dashed line; in comparison, the 283–361 mutant shows a markedly different behaviour (dotted line). WT, wild-type. (**B**) A summary of the calculated activation energy values ($E_{act,app}$) is shown. The dotted line corresponds to the value calculated for the AT_{C232S} control; 283–361 and 292–339 were found to be significantly different from the control ($P < 0.001$ and $P < 0.05$ respectively) by one-way ANOVA with Bonferroni correction. (**C**) Half-times of polymerization at 55 °C (●), 60 °C (■) and 65 °C (▲) are shown in relation to the T_m values of the variants. The dashed lines represent the dependence of polymerization on experimental temperature and T_m in the presence of osmolytes, using the data presented in Figure 3. (**D**) Notional energy landscapes of the progression from the native conformation, N, to the partially unfolded intermediate, I, via the transition state of the irreversible step, ‡, culminating in polymer formation, P. The solid line represents the 'wild-type' scenario, whereas the broken line indicates possible alternate changes to the pathway resulting in a reduction in polymer formation. Results are means ± S.E.M.

pathway. Of the mutants considered in the present study, only 283–361 has a pronounced destabilizing effect on the kinetically controlled step.

Re-appraisal of published rates of polymerization for mutants of α_1-antitrypsin

Several studies have previously characterized stabilized and destabilized mutants of α_1-antitrypsin. For a combined analysis, five published datasets are considered in the present study [28,29,49–51]; when combined with the 60 °C data described in the present paper, this represents 36 unique mutants. These datasets differ in the manner in which T_m value was determined (CD and SYPRO Orange), the T_m value reported for the wild-type control, the temperature at which polymerization was recorded (45 °C, 52 °C and 60 °C) and the means by which it was monitored (tryptophan fluorescence and non-denaturing PAGE analysis). By way of comparison, a further 12 are considered separately, from
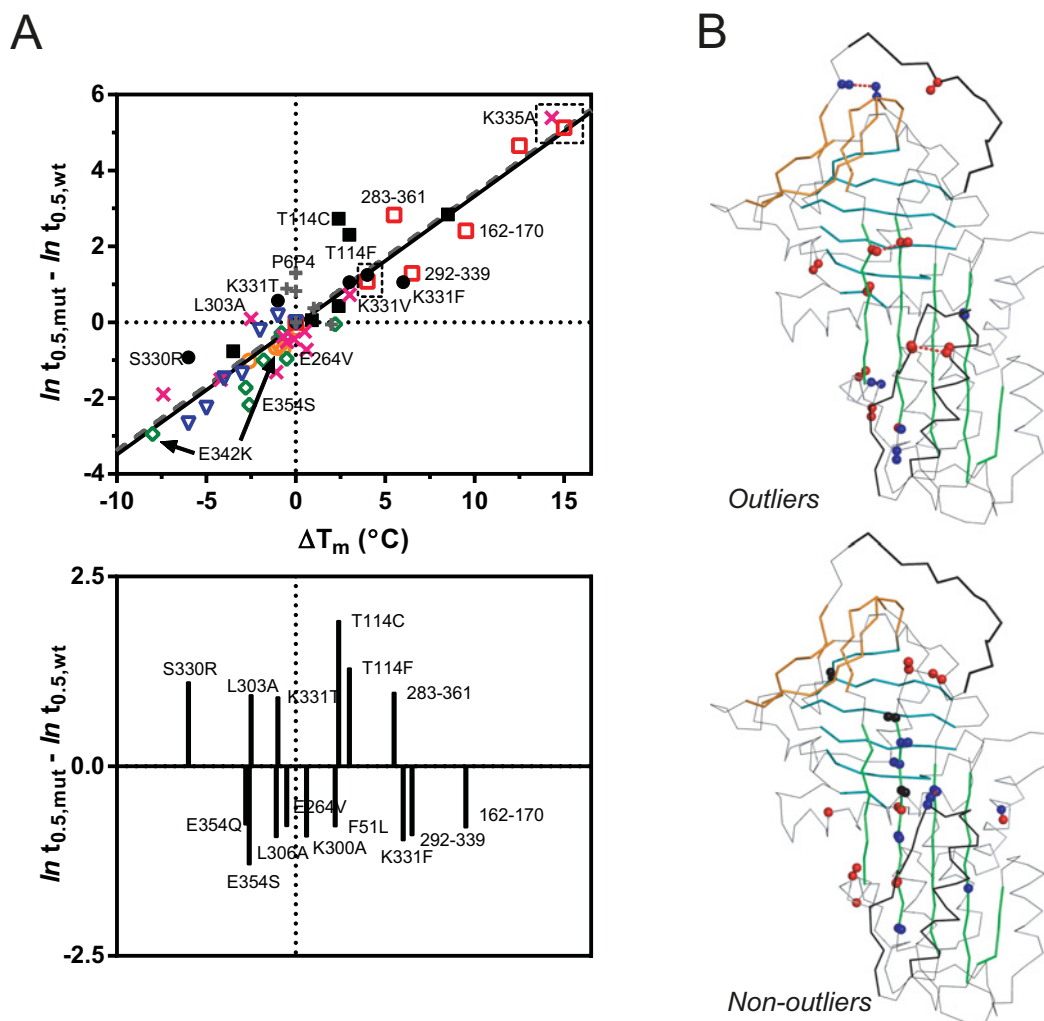
a study in which rates were obtained from the change in bis-ANS fluorescence [52], and one in which mutants were intentionally designed to interfere with polymerization but not stability [36]. As shown in the present study, due to the apparent Arrhenius-type dependence of the polymerization rate on temperature, it was possible to normalize the $t_{0.5}$ values by reporting them as the absolute difference to the natural logarithm of the wild-type control under the specific conditions of each experiment. Similarly, transition midpoints could be reported as ΔT_m values relative to the wild-type control.

The combined result is shown in the upper panel of Figure 6(A). Although there are clear deviations from the overall trend, the Figure highlights that the rate of polymerization is overwhelmingly determined by the thermal stability of the native state for both stabilizing and destabilizing variants. Remarkably, when a linear regression was performed of the data, there was a virtually identical correspondence with the relationship between osmolyte-mediated stabilization and rate of polymerization (Figure 6A, upper panel, dashed line).

Table 4 Polymerization of the α_1-antitrypsin variants

The times taken to reach a half-maximal polymerization FRET signal (in s) at the different assay temperatures are shown, with the standard error calculated from at least five independent experiments, along with the calculated apparent activation energy of the reaction. The P values for mutants with a significantly different E_{act} value to wild-type (based on a multiple one-way ANOVA comparison with AT_{C232S} using Bonferroni's correction) are indicated. n.s, not significant.

| Variant | Temperature | | | E_{act} (kJ/mol) | Significance |
	55°C	60°C	65°C		
AT_{C232S}	880 ± 127	109 ± 9	38 ± 7	298 ± 10	–
162–170	$3.93 \, (\pm 0.09) \times 10^3$	941 ± 41	226 ± 7	262 ± 6	n.s.
168–189	$21.9 \, (\pm 1.7) \times 10^3$	$8.87 \, (\pm 0.34) \times 10^3$	$1.01 \, (\pm 0.05) \times 10^3$	283 ± 16	n.s.
283–361	$8.97 \, (\pm 0.96) \times 10^3$	$1.43 \, (\pm 0.23) \times 10^3$	37 ± 8	482 ± 32	$P < 0.001$
292–339	$2.29 \, (\pm 0.20) \times 10^3$	307 ± 56	51 ± 3	354 ± 21	$P < 0.05$
K331V	$1.31 \, (\pm 0.07) \times 10^3$	248 ± 9	39 ± 1	322 ± 6	n.s.
K335A	$40.4 \, (\pm 3.2) \times 10^3$	$14.2 \, (\pm 1.0) \times 10^3$	$2.52 \, (\pm 0.10) \times 10^3$	261 ± 13	n.s.

Figure 6 Combined retrospective analysis

(**A**) The top panel presents an analysis of the relationship between polymerization kinetics and T_m value compiled from six studies: Dafforn et al. [28] (green open diamonds), Parfrey et al. [49] (black closed squares), Gilis et al. [29] (black closed circles), Knaupp et al. [51] (orange open circles), Knaupp et al. [50] (pink crosses), and the mutants described in the present study (red open squares). In addition, included by way of comparison, are values determined by Cabrita et al. [52] (blue open triangles) using bis-ANS and Haq et al. [36] (grey crosses) using RCL mutants. The sets of data differed in the manner in which T_m values were determined, the T_m reported for the wild-type control and the temperature and means by which polymerization was monitored. The half-times and ΔT_m values were normalized relative to the values for the wild-type control as determined in each study. The solid line indicates the linear regression performed using the six datasets; the broken line shows the relationship determined using osmolytes (from Figure 3D). The lower panel presents shortlisted mutants for which the magnitude of difference in $\ln(t_{0.5})$ from the trend line exceeded ± 0.75 units. (**B**) The upper panel shows the same select mutants, mapped on to the structure of α_1-antitrypsin using PyMOL. Blue spheres indicate less ability to polymerize than predicted and red spheres indicate higher rates of polymerization than predicted from ΔT_m. The lower panel indicates mutants for which the rate of polymerization is consistent with the expected value; red spheres denote those for which ΔT_m is negative (destabilizing) and blue designates a positive ΔT_m (stabilizing).

Of particular interest, is the ability to identify outliers to the curve, shown in the lower panel of Figure 6(A) and mapped on to the structure of α_1-antitrypsin in Figure 6(B). These are mutants that affect polymerization, either positively or negatively, in a manner that is not completely accounted for by the stability of the native state. In particular, mutants increasing the packing of a 'pocket' situated proximal to the F-helix, at Thr[114] [61], resist polymerization to a greater extent than would be predicted from the model. Conversely, the loss of the salt bridge mediated by Glu[354] of the RCL promotes polymerization to a greater degree than expected, possibly for the same reason that 283–361 disfavours it. RCL mutants designed to interfere specifically with the polymerization mechanism also show an atypically decreased rate. Although not providing the level of detail that multiple temperature experiments can, the ability to identify outliers to the normalized stability-polymerization curve is useful for pinpointing mutations that affect the stability of non-native components of the pathway.

Summary

The present study concerns the means by which polymerization is perturbed by mutation: the relative contribution of specific effects on the underlying structural mechanism and non-specific effects on protein stability. The remarkable congruence between additive-induced and mutation-induced effects on polymerization strongly suggests that changes in global stability are the dominant factor.

This result has clear relevance to the characterization of polymer-generating serpins. Although a general trend has been noted in other studies, the extent and consistency of the underlying interrelationship between stability and polymerization has been under-appreciated in the literature. On the basis of the present study, it is evident that in the absence of more refined approaches, an increase in resistance to polymerization is of itself insufficient to support interpretations related to the underlying mechanism. It is suggested that quantification of the deviation from the described correlation, coupled with a multiple-temperature analysis, should be performed to ascertain the degree to which changes in global stability influence the outcome of any such experiment.

AUTHOR CONTRIBUTION

James Irving, Imran Haq, Jennifer Dickens and Sarah Faull designed and performed the experiments and analysed the data. David Lomas and James Irving directed the research. James Irving and David Lomas wrote the paper. All authors contributed revisions to, and approved, the final version of the paper.

FUNDING

REFERENCES

1   Silverman, G. A., Bird, P. I., Carrell, R. W., Church, F. C., Coughlin, P. B., Gettins, P., Irving, J., Lomas, D. A., Moyer, R. W., Pemberton, P. et al. (2001) The serpins are an expanding superfamily of structurally similar but functionally diverse proteins. Evolution, novel functions, mechanism of inhibition and a revised nomenclature. J. Biol. Chem. **276**, 33293–33296

2   Irving, J. A., Steenbakkers, P. J. M., Lesk, A. M., Op den Camp, H. J. M., Pike, R. N. and Whisstock, J. C. W. (2002) Serpins in prokaryotes. Mol. Biol. Evol. **19**, 1881–1890

3   Anfinsen, C. B. (1973) Principles that govern the folding of protein chains. Science **181**, 223–230

4   Whisstock, J. C. and Bottomley, S. P. (2006) Molecular gymnastics, serpin structure, folding and misfolding. Curr. Opin. Struct. Biol. **16**, 761–768

5   Stein, P. E. and Carrell, R. W. (1995) What do dysfunctional serpins tell us about molecular mobility and disease? Nat. Struct. Biol. **2**, 96–113

6   Lomas, D. A., Evans, D. L., Finch, J. T. and Carrell, R. W. (1992) The mechanism of Z α_1-antitrypsin accumulation in the liver. Nature **357**, 605–607

7   Lomas, D. A., Finch, J. T., Seyama, K., Nukiwa, T. and Carrell, R. W. (1993) α_1-Antitrypsin Siiyama (Ser53→Phe). Further evidence for intracellular loop-sheet polymerization. J. Biol. Chem. **268**, 15333–15335

8   Mast, A. E., Enghild, J. J. and Salvesen, G. (1992) Conformation of the reactive site loop of α_1-proteinase inhibitor probed by limited proteolysis. Biochemistry **31**, 2720–2728

9   Elliott, P. R., Bilton, D. and Lomas, D. A. (1998) Lung polymers in Z α_1-antitrypsin deficiency-related emphysema. Am. J. Respir. Cell Mol. Biol. **18**, 670–674

10   Lomas, D. A. and Mahadeva, R. (2002) α_1-Antitrypsin polymerisation and the serpinopathies: pathobiology and prospects for therapy. J. Clin. Invest. **110**, 1585–1590

11   Gooptu, B. and Lomas, D. A. (2008) Polymers and inflammation: disease mechanisms of the serpinopathies. J. Exp. Med. **205**, 1529–1534

12   Ekeowa, U. I., Gooptu, B., Belorgey, D., Hägglöf, P., Karlsson-Li, S., Miranda, E., Pérez, J., MacLeod, I., Kroger, H., Marciniak, S. J. et al. (2009) α_1-Antitrypsin deficiency, chronic obstructive pulmonary disease and the serpinopathies. Clin. Sci. **116**, 837–850

13   Davis, R. L., Shrimpton, A. E., Holohan, P. D., Bradshaw, C., Feiglin, D., Collins, G. H., Sonderegger, P., Kinter, J., Becker, L. M., Lacbawan, F. et al. (1999) Familial dementia caused by polymerization of mutant neuroserpin. Nature **401**, 376–379

14   Gooptu, B. and Lomas, D. A. (2009) Conformational pathology of the serpins: themes, variations and therapeutic strategies. Annu. Rev. Biochem. **78**, 147–176

15   Devlin, G. L., Chow, M. K. M., Howlett, G. J. and Bottomley, S. P. (2002) Acid denaturation of a1-antitrypsin: characterization of a novel mechanism of serpin polymerization. J. Mol. Biol. **324**, 859–870

16   Sivasothy, P., Dafforn, T. R., Gettins, P. G. and Lomas, D. A. (2000) Pathogenic α_1-antitrypsin polymers are formed by reactive loop-β-sheet A linkage. J. Biol. Chem. **275**, 33663–33668

17   Huntington, J. A., Pannu, N. S., Hazes, B., Read, R. J., Lomas, D. A. and Carrell, R. W. (1999) A 2.6 Å structure of a serpin polymer and implications for conformational disease. J. Mol. Biol. **293**, 449–455

18   Dunstone, M. A., Dai, W., Whisstock, J. C., Rossjohn, J., Pike, R. N., Feil, S. C., Le Bonniec, B. F., Parker, M. W. and Bottomley, S. P. (2000) Cleaved antitrypsin polymers at atomic resolution. Protein Sci. **9**, 417–420

19   Krishnan, B. and Gierasch, L. M. (2011) Dynamic local unfolding in the serpin α_1 antitrypsin provides a mechanism for loop insertion and polymerization. Nat. Struct. Mol. Biol. **18**, 222–226

20   Nyon, M. P., Segu, L., Cabrita, L. D., Lévy, G. R., Kirkpatrick, J., Roussel, B. D., Patschull, A. O., Barrett, T. E., Ekeowa, U. I., Kerr, R. et al. (2012) Structural dynamics associated with intermediate formation in an archetypal conformational disease. Structure **20**, 504–512

21   Yamasaki, M., Li, W., Johnson, D. J. and Huntington, J. A. (2008) Crystal structure of a stable dimer reveals the molecular basis of serpin polymerization. Nature **455**, 1255–1258

22   Yamasaki, M., Sendall, T. J., Pearce, M. C., Whisstock, J. C. and Huntington, J. A. (2011) Molecular basis of α_1-antitrypsin deficiency revealed by the structure of a domain-swapped trimer. EMBO Rep. **12**, 1011–1017

23   Powell, L. M. and Pain, R. H. (1992) Effects of glycosylation on the folding and stability of human, recombinant and cleaved α_1-antitrypsin. J. Mol. Biol. **224**, 241–252

24   James, E. L., Whisstock, J. C., Gore, M. G. and Bottomley, S. P. (1999) Probing the unfolding pathway of α_1-antitrypsin. J. Biol. Chem. **274**, 9482–9488

25   Lomas, D. A., Evans, D. L., Stone, S. R., Chang, W. S. and Carrell, R. W. (1993) Effect of the Z mutation on the physical and inhibitory properties of α_1-antitrypsin. Biochemistry **32**, 500–508

26   Miranda, E., Perez, J., Ekeowa, U. I., Hadzic, N., Kalsheker, N., Gooptu, B., Portmann, B., Belorgey, D., Hill, M., Chambers, S. et al. (2010) A novel monoclonal antibody to characterize pathogenic polymers in liver disease associated with α_1-antitrypsin deficiency. Hepatology **52**, 1078–1088

27   Ekeowa, U. I., Freeke, J., Miranda, E., Gooptu, B., Bush, M. F., Perez, J., Teckman, J., Robinson, C. V. and Lomas, D. A. (2010) Defining the mechanism of polymerization in the serpinopathies. Proc. Natl. Acad. Sci. U.S.A. **107**, 17146–17151

28   Dafforn, T. R., Mahadeva, R., Elliott, P. R., Sivasothy, P. and Lomas, D. A. (1999) A kinetic mechanism for the polymerization of α_1-antitrypsin. J. Biol. Chem. **274**, 9548–9555

29   Gilis, D., McLennan, H. R., Dehouck, Y., Cabrita, L. D., Rooman, M. and Bottomley, S. P. (2003) *In vitro* and *in silico* design of α_1-antitrypsin mutants with different conformational stabilities. J. Mol. Biol. **325**, 581–589

30 Chang, W. S., Whisstock, J. C., Hopkins, P. C., Lesk, A. M., Carrell, R. W. and Wardell, M. R. (1997) Importance of the release of strand 1C to the polymerization mechanism of inhibitory serpins. Protein Sci. **6**, 89–98

31 Baek, J. H., Im, H., Kang, U. B., Seong, K. M., Lee, C., Kim, J. and Yu, M. H. (2007) Probing the local conformational change of α_1-antitrypsin. Protein Sci. **16**, 1842–1850

32 Fass, D. (2012) Disulfide bonding in protein biophysics. Annu. Rev. Biophys. **41**, 63–79

33 Chow, M. K. M., Devlin, G. L. and Bottomley, S. P. (2001) Osmolytes as modulators of conformational changes in the serpins. Biol. Chem. **382**, 1593–1599

34 Sharp, L. K., Mallya, M., Kinghorn, K. J., Wang, Z., Crowther, D. C., Huntington, J. A., Belorgey, D. and Lomas, D. A. (2006) Sugar and alcohol molecules provide a therapeutic strategy for the serpinopathies that cause dementia and cirrhosis. FEBS J. **273**, 2540–2552

35 Devlin, G. L., Parfrey, H., Tew, D. J., Lomas, D. A. and Bottomley, S. P. (2001) Prevention of polymerization of M and Z α_1-antitrypsin (α_1-AT) with trimethylamine N-oxide. Implications for the treatment of α_1-AT deficiency. Am. J. Respir. Cell Mol. Biol. **24**, 727–732

36 Haq, I., Irving, J. A., Faull, S. V., Dickens, J. A., Ordonez, A., Belorgey, D., Gooptu, B. and Lomas, D. A. (2013) Reactive centre loop mutants of α_1-antitrypsin reveal position-specific effects on intermediate formation along the polymerization pathway. Biosci. Rep. **33**, e00046

37 Hoops, S., Sahle, S., Gauges, R., Lee, C., Pahle, J., Simus, N., Singhal, M., Xu, L., Mendes, P. and Kummer, U. (2006) COPASI: a COmplex PAthway SImulator. Bioinformatics **22**, 3067–3074

38 Zhou, A., Carrell, R. W. and Huntington, J. A. (2001) The serpin inhibitory mechanism is critically dependent on the length of the reactive center loop. J. Biol. Chem. **276**, 27541–27547

39 Im, H., Seo, E. J. and Yu, M.-H. (1999) Metastability in the inhibitory mechanism of human α_1-antitrypsin. J. Biol. Chem. **274**, 11072–11077

40 Riener, C. K., Kada, G. and Gruber, H. J. (2002) Quick measurement of protein sulfhydryls with Ellman's reagent and with 4,4'-dithiodipyridine. Anal. Bioanal. Chem. **373**, 266–276

41 Nettleship, J. E., Brown, J., Groves, M. R. and Geerlof, A. (2008) Methods for protein characterization by mass spectrometry, thermal shift (ThermoFluor) assay, and multiangle or static light scattering. Methods Mol. Biol. **426**, 299–318

42 Lawrence, D. A., Olson, S. T., Palaniappan, S. and Ginsburg, D. (1994) Engineering plasminogen activator inhibitor 1 mutants with increased functional stability. Biochemistry **33**, 3643–3648

43 Reference deleted

44 Zhou, A. and Carrell, R. W. (2008) Dimers initiate and propagate serine protease inhibitor polymerisation. J. Mol. Biol. **375**, 36–42

45 Friedler, A., Veprintsev, D. B., Hansson, L. O. and Fersht, A. R. (2003) Kinetic instability of p53 core domain mutants: implications for rescue by small molecules. J. Biol. Chem. **278**, 24108–24112

46 Reference deleted

47 Kezdy, F. J. and Kaiser, E. T. (1970) Principles of active site titration of proteolytic enzymes. Methods Enzymol. **19**, 3–20

48 Hopkins, P. C., Carrell, R. W. and Stone, S. R. (1993) Effects of mutations in the hinge region of serpins. Biochemistry **32**, 7650–7657

49 Parfrey, H., Mahadeva, R., Ravenhill, N. A., Zhou, A., Dafforn, T. R., Foreman, R. C. and Lomas, D. A. (2003) Targeting a surface cavity of α_1-antitrypsin to prevent conformational disease. J. Biol. Chem. **278**, 33060–33066

50 Knaupp, A. S., Keleher, S., Yang, L., Dai, W., Bottomley, S. P. and Pearce, M. C. (2013) The roles of helix I and strand 5A in the folding, function and misfolding of α_1-antitrypsin. PLoS ONE **8**, e54766

51 Knaupp, A. S. and Bottomley, S. P. (2011) Structural change in beta-sheet A of Z α_1-antitrypsin is responsible for accelerated polymerization and disease. J. Mol. Biol. **413**, 888–898

52 Cabrita, L. D., Dai, W. and Bottomley, S. P. (2004) Different conformational changes within the F-helix occur during serpin folding, polymerization and proteinase inhibition. Biochemistry **43**, 9834–9839

53 Pace, C. N. and Scholtz, J. M. (1997) Measuring the conformational stability of a protein. In Protein Structure: A Practical Approach (Creighton, T. E., ed.), pp. 299–321, Oxford University Press, Oxford

54 Niesen, F. H., Berglund, H. and Vedadi, M. (2007) The use of differential scanning fluorimetry to detect ligand interactions that promote protein stability. Nat. Protoc. **2**, 2212–2221

55 Koloczek, H., Banbula, A., Salvesen, G. S. and Potempa, J. (1996) Serpin α_1-proteinase inhibitor probed by intrinsic tryptophan fluorescence spectroscopy. Protein Sci. **5**, 2226–2235

56 Sanchez-Ruiz, J. M. (2010) Protein kinetic stability. Biophys. Chem. **148**, 1–15

57 Cox, D. W., Billingsley, G. D. and Callahan, J. W. (1986) Aggregation of plasma Z type α_1-antitrypsin suggests basic defect for the deficiency. FEBS Lett. **205**, 255–260

58 Harries, D. and Rosgen, J. (2008) A practical guide on how osmolytes modulate macromolecular properties. Methods Cell Biol. **84**, 679–735

59 Costas, M., Rodriguez-Larrea, D., De Maria, L., Borchert, T. V., Gomez-Puyou, A. and Sanchez-Ruiz, J. M. (2009) Between-species variation in the kinetic stability of TIM proteins linked to solvation-barrier free energies. J. Mol. Biol. **385**, 924–937

60 Simonovic, I. and Patston, P. A. (2000) The native metastable fold of C1-inhibitor is stabilized by disulfide bonds. Biochim. Biophys. Acta **1481**, 97–102

61 Gooptu, B., Miranda, E., Nobeli, I., Mallya, M., Purkiss, A., Leigh Brown, S. C., Summers, C., Phillips, R. L., Lomas, D. A. and Tracey, B. E. (2009) Crystallographic and cellular characterisation of two mechanisms stabilising the native fold of α_1-antitrypsin: implications for disease and drug design. J. Mol. Biol. **387**, 857–868

62 Elliott, P. R., Pei, X. Y., Dafforn, T. R. and Lomas, D. A. (2000) Topography of a 2.0 Å structure of α_1-antitrypsin reveals targets for rational drug design to prevent conformational disease. Protein Sci. **9**, 1274–1281

SUPPLEMENTARY ONLINE DATA
Altered native stability is the dominant basis for susceptibility of α_1-antitrypsin mutants to polymerization

James A. IRVING*[1,2], Imran HAQ†[1], Jennifer A. DICKENS*, Sarah V. FAULL* and David A. LOMAS†

*Cambridge Institute for Medical Research, Department of Medicine, University of Cambridge, Wellcome Trust/MRC Building, Hills Road, Cambridge CB2 0XY, U.K.
†Wolfson Institute for Biomedical Research, The Cruciform Building, University College London, Gower Street, London WC1E 6BT, U.K.

EXPERIMENTAL

Derivation of eqn (3)

Eqn (2) in the main text reflects the approximately linear dependence of the difference in log half-times on ΔT_m value when comparing stabilized and control α_1-antitrypsin preparations. This represents an approximation of eqn (1), which, despite describing a hyperbolic relationship, is almost linear in nature over the range of temperatures considered (Figures 3A–3C of the main text). If we compare the natural logarithm of $t_{0.5,\text{stab}}$ of a stabilized protein with respect to that of the control, $t_{0.5,\text{wt}}$, the result is independent of experimental temperature, T. From eqn (1):

$$\ln(t_{0.5,\text{stab}}) - \ln(t_{0.5,\text{wt}})$$
$$= (E_{\text{act,app}}/R)\,(1/T - 1/T^*_{\text{stab}})$$
$$\quad - (E_{\text{act,app}}/R)(1/T - 1/T^*_{\text{wt}})$$
$$= -(E_{\text{act,app}}/R)\,(1/T^*_{\text{stab}} - 1/T^*_{\text{wt}})$$
$$= (E_{\text{act,app}}/R)\,(T^*_{\text{stab}} - T^*_{\text{wt}})/(T^*_{\text{stab}}T^*_{\text{wt}}) \qquad \text{(S1)}$$

where, as explained in the text, T^* is a reference temperature at which the rate of polymerization is $1\ \text{s}^{-1}$. For a difference $\Delta T^* = T^*_{\text{stab}} - T^*_{\text{wt}}$, it follows that:

$$\ln(t_{0.5,\text{stab}}) - \ln(t_{0.5,\text{wt}}) = (E_{\text{act,app}}\Delta T^*)/\left[RT^*_{\text{wt}}(T^*_{\text{wt}}+\Delta T^*)\right] \quad \text{(S2)}$$

As T^* values are reported in Kelvin, for the relevant experimentally determined values, $\Delta T^* < 0.1 \times T^*_{\text{wt}}$. At small values of ΔT^* therefore, the equation simplifies to:

$$\ln(t_{0.5,\text{stab}}) - \ln(t_{0.5,\text{wt}}) \approx (E_{\text{act,app}}\Delta T^*)/(RT^{*2}_{\text{wt}}) \qquad \text{(S3)}$$

and if $T^*_{\text{wt}} = aT_{\text{m,wt}}$,

$$\ln(t_{0.5,\text{stab}}) - \ln(t_{0.5,\text{wt}}) \approx (E_{\text{act,app}}\Delta T_{\text{m}})/(aRT_{\text{m,wt}}^2) \qquad \text{(S4)}$$

For values $E_{\text{act,app}} = 3.20 \times 10^3$ kJ/mol, $a = 1.05$ and $T_{\text{m,wt}} = 55\,°\text{C}$, calculated from the experimental data. $E_{\text{act,app}}/aRT_{\text{m,wt}}^2 = 0.34$, which is identical with the slope of the linear regression calculated from the experimental data and presented in eqn (2).

---

[1] These authors contributed equally to this work.
[2] To whom correspondence should be addressed at the present address: Wolfson Institute for Biomedical Research, The Cruciform Building, University College London, Gower Street, London WC1E 6BT, U.K. (email j.irving@ucl.ac.uk).
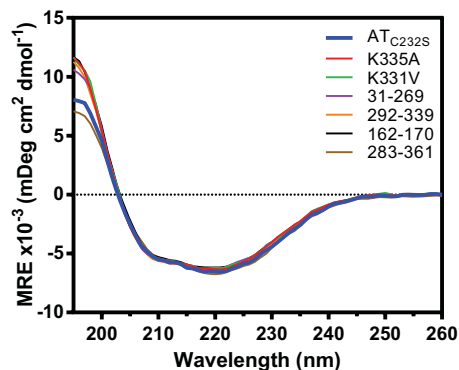
Figure S1   Recombinant mutant CD spectra

The normalized CD spectra of the mutants considered in the present study were recorded between 260 nm and 190 nm in 10 mM Na_2HPO_4/NaH_2PO_4 (pH 7.4) buffer, and show a similar shape to that of the wild-type protein (blue).
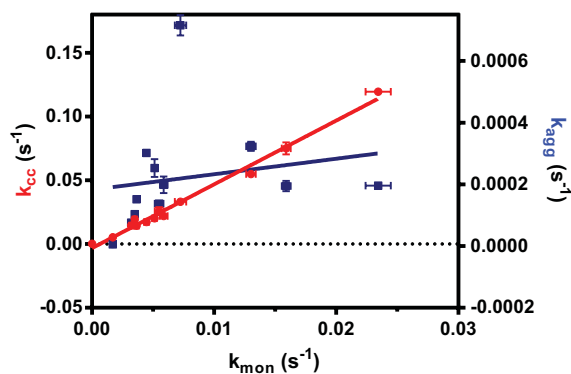

Figure S2   Comparison of polymerization parameters determined by non-denaturing PAGE and bis-ANS fluorescence

All values are taken from Knaupp et al. [1]. The reported rate of disappearance of monomeric α_1-antitrypsin evaluated by non-denaturing PAGE (k_{mon}) is shown in comparison with the initial rapid rate of increase in bis-ANS fluorescence (k_{cc}; red) and subsequent slow decrease (k_{agg}; blue) for several α_1-antitrypsin variants. There is a strong linear correspondence ($R^2 = 0.99$) between gel densitometry and the rapid initial increase in bis-ANS fluorescence, but not between gel densitometry and the slow phase ($R^2 = 0.03$).

Table S1   Optimal parameters obtained from the non-linear regression analysis of T_m and polymerization half-time

Values were calculated for the apparent activation energy $E_{act,app}$ and scaling factor a in the presence of TMAO, sucrose and sodium sulfate. Standard errors of a were < 1%.

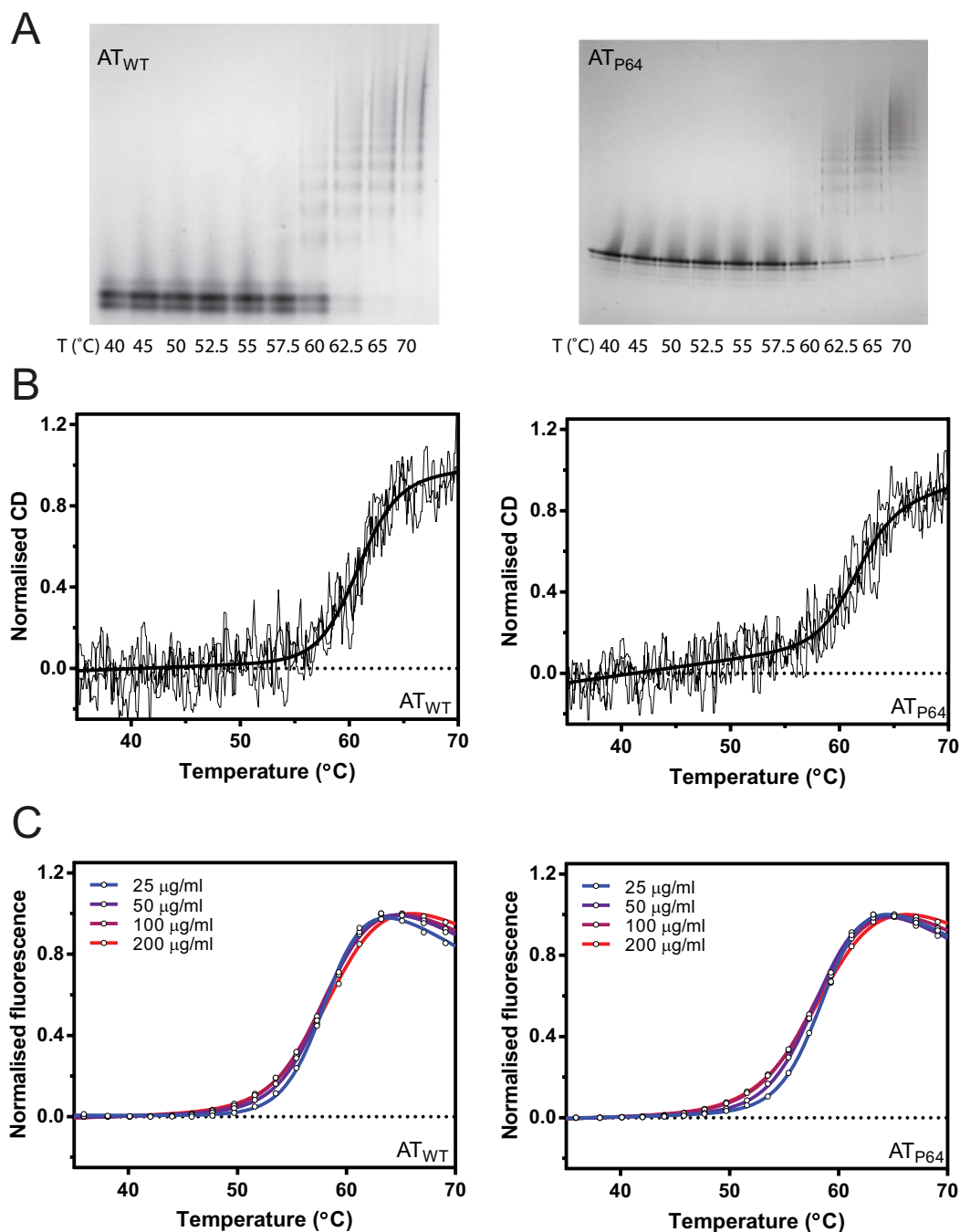| Additive	$E_{act,app}$ (kJ/mol)	a
All (combined)	320 ± 4	1.05
TMAO	328 ± 6	1.05
Sucrose	318 ± 8	1.05
Sodium sulfate	317 ± 7	1.05

Figure S3   Processes forming the basis of thermal unfolding profiles

(**A**) A typical non-denaturing PAGE profile, with aliquots of recombinant α_1-antitrypsin (left-hand panel) removed over the course of a CD-based thermal unfolding experiment. The concentration was 0.1 mg/ml and the sample was heated at 1°C/min; the prevailing sample temperature is indicated. The gel was visualized using Coomassie Blue. The same experiment performed using the less polymerization-prone AT_{P64} variant is shown in the right-hand panel. (**B**) The fit of the two-state unfolding curves, reported in Figure 1(E) of the main text, to normalized CD data read at 225 nm, for AT_{WT} (left-hand panel) and AT_{P64} (right-hand panel). The temperature was increased at a rate of 5°C/min and the protein concentration was 0.025 mg/ml. Data from three independent experiments are shown. (**C**) Thermal unfolding profiles from two independent experiments, measured as a function of increase in SYPRO Orange fluorescence of AT_{WT} (left-hand panel) and AT_{P64} (right-hand panel). Samples at 0.025, 0.05, 0.1 and 0.2 mg/ml were heated at a rate of 5°C/min, with slight variation of profile shape, but almost identical transition midpoints.
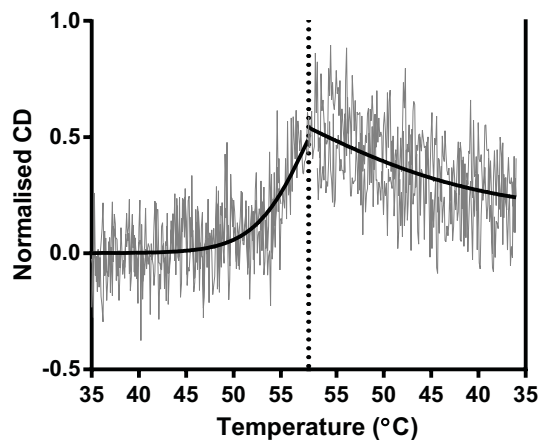
Figure S4   Partial reversibility of temperature-induced change in CD at 225 nm

Recombinant α_1-antitrypsin, at a concentration of 0.1 mg/ml, was heated at a rate of 1 °C/min to 58 °C, approximately the transition midpoint, and cooled at the same rate. The profile shows partial recovery of the initial CD value. Sample temperature was monitored directly using a submerged thermistor probe. Data are from two independent experiments.

REFERENCE

1   Knaupp, A. S., Keleher, S., Yang, L., Dai, W., Bottomley, S. P. and Pearce, M. C. (2013) The roles of helix I and strand 5A in the folding, function and misfolding of α_1-antitrypsin. PLoS ONE **8**, e54766